Control of a Multi-functional Solar PV-Battery System for Operation in a Microgrid Environment

Brijendra Kumar Verma, Sachin Devassy, Subhash Kumar Ram, Anand Abhishek, Ajeet Dhakar
Power Electronics Group
CSIR-CEERI, Pilani
Rajasthan-333031, India

Abstract—**This work deals with the control and operation of a multi-functional PV-Battery Integrated System operating in a Micro-grid environment. The system consists of a three-phase three wire PV array and battery Integrated distribution static compensator (PV-B-DSTATCOM) which can not only compensate for current quality issues due to load current but also inject power from the PV array into the grid. A battery bank is also integrated with the PV system so as to enable its operation in standalone mode of operation when grid is not available or under faulty conditions. This system is critical in modern distribution systems which require clean source of energy along with continuous supply of power for sophisticated electronic loads for data centres, hospitals and electronic industries. The system performance is extensively evaluated under various dynamic conditions such as irradiation variation, load unbalance and also operation in standalone and grid connected mode of operation.**

Index Terms—**Energy Storage, Active filter, Maximum power point tracking, Power quality, Solar photovoltaic system, micro-grid.**

I. Introduction

THE need for clean energy and good power quality has been on fore front in modern distribution systems. This has led to extensive research to incorporate functionality of a conventional solar grid tied inverter as well as active power filter into a single multi-functional system [1], [2]. The need for improved power quality is fueled by the increased usage of sophisticated electronic systems used in computer data servers, hospital equipments, semiconductor industries etc. These systems draw nonlinear currents due to the switching devices such as MOSFETs and IGBTs incorporated in these system. The nonlinear currents cause distortion of voltage at the point of common coupling which can affect nearby local loads along with heating of distribution transformers etc. [3], [4]. Integration of battery energy storage along with PV system enables the uninterrupted operation of the system. This functionality is critical there is frequent interruption in power supplies such as in remote locations far from major cities.

A number of research work has been carried out in the area of PV integrated shunt compensator systems. The extraction of fundamental component of nonlinear signal is a major task in control of PV-Battery Integrated shunt compensator systems [5]. A technique for extraction of fundamental component of distorted voltage using multiple complex coefficient filter is presented in [6]. Though this technique has excellent performance, it has significant computational burden. Adaptive filtering is an another technique for extracting the fundamental component of a distorted load signal. A number of techniques based on least square means (LMS) and its variants, recursive least square means (RLS) and its variants have been proposed for control of distributed static compensators (DSTATCOM) [7], [8]. These methods however these methods have weight factors which needs to be adjusted based on convergence speed and steady state error.

Since operation in both standalone and grid connected mode of operation is critical in microgrid operation, seamless transistion between these modes is essential so that the sophisticated loads do not affected due to frequent power failures. In [9], [10], seamless transition between standalone operation of PV inverters and grid connected operation has been presented. This work presents the control operation of a multi-functional PV-Battery Shunt compensator operating in a micro-grid environment. The system consists of a three phase VSI in which the PV array is directly integrated at the DC-link of the system. The battery bank is linked to the DC-link of the system through a bi-directional DC-DC converter. The bi-directional controller maintains the DC-bus of the system and maintains it at a level such that PV array is operated at its maximum power point condition. In grid connected condition, the shunt compensator operates in current control mode and compensates for load current quality issues and also injects power from PV array into the grid. During conditions of grid fault conditions, the shunt compensator automatically transits to standalone mode of operation and operates in voltage control mode, supplying a regulated AC voltage supply for the load. The system performance is evaluated through extensive simulation in Matlab-Simulink Environment. The performance of the system is tested under conditions of irradiation variation, load unbalance and grid fault conditions.

II. System Configuration and Design

The system configuration of three phase three wire solar PV array and battery integrated dstatcom (PV-B-DSTATCOM) is presented in 1.

The system consists of a three phase DSTATCOM connected in a three phase three wire distribution system. The load consists of nonlinear sensitive loads. The solar PV array is integrated at the DC-link of the DSTATCOM. A bidirectional DC-DC converter is used to integrate the battery bank with the shunt compensator systems. The PV-B-DSTATCOM is interfaced with supply system through interfacing inductors

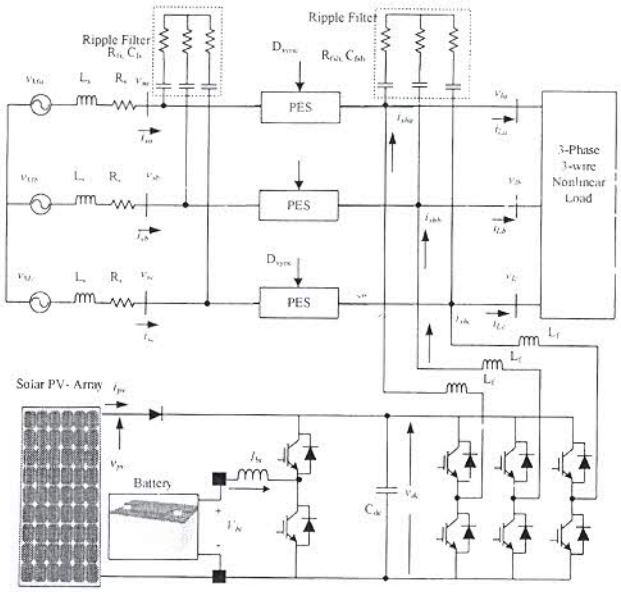

Fig. 1. System Configuration PV-B-DSTATCOM

(Lr). A power electronic switch (PES) is used to disconnect the PCC from the PV-B-DSTATCOM during conditions of grid fault conditions so that the system. There are ripple filters before and after the PES to mitigate high frequency switching harmonics.

III. Control of PV-B-DSTATCOM

The PV-B-DSTATCOM system has two major subsystems namely bidirectional DC-DC converter and DSTATCOM. There are two modes of operation namely grid connected and standalone mode of operation. The control of these systems are presented in the following sections.

A. Control of Bidirectional DC-DC converter

The Bidirectional DC-DC converter integrates the battery energy storage with the DC-link of the system. The reference voltage for the DC-link of the system is obtained through maximum power point tracking algorithm. The maximum power point algorithm used in this work is perturb and observe algorithm. The reference DC-link voltage is given

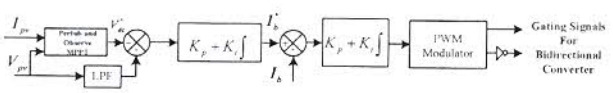

Fig. 2. Control of Bidirectional Converter

to a proportional integral (PI) controller which then gives reference battery current. The difference between the reference battery current (I_b^*) and actual battery current is given to a PI controller to generate gating signals for the bidirectional DC-DC converter.

B. Control of DSTATCOM system

C. Phase generation and Synchronization Control

The PV-B-DSTATCOM operates in voltage control mode during the standalone mode of operation and in current control mode during grid connected mode of operation When the difference between the reference load voltage and PCC voltage (v_s^*) is more than 0.2 pu, then a fixed frequency (f_s^*) is used to generate the phase of the PV-B-DSTATCOM. As soon as grid voltage is more than 0.8pu, the phase generation loop tries to match the phase of load voltage with PCC voltage through a phase PI loop which generates change in frequency signal. This signal is added with actual load frequency and then passed to integrator to generate the phase of the load voltage.

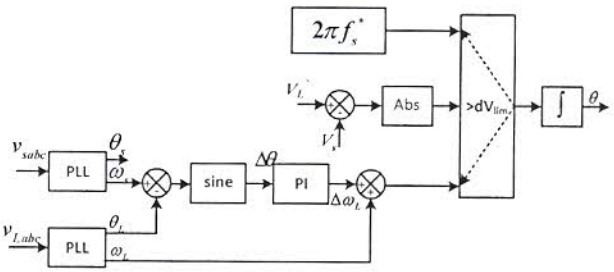

Fig. 3. Phase Generation in Bidirectional PV-B-DSTATCOM

The synchronization logic works on consideration of three parameters, phase difference between PCC voltage and load voltage ($\Delta\theta$), difference between nominal frequency f_s^* and grid frequency f_s and magnitude difference between reference load voltage V_L^* and PCC voltage V_s. The phase difference $\Delta\theta$ should be less than 3 degrees, frequency difference should be less than 0.3 Hz, magnitude difference should be less than 0.05 pu. When all these conditions are met simultaneously, the resultant logic signal (D_{sync}) is 1 which is then used to turn-on the PES as well as change mode of operation from standalone mode to grid connected mode of operation.

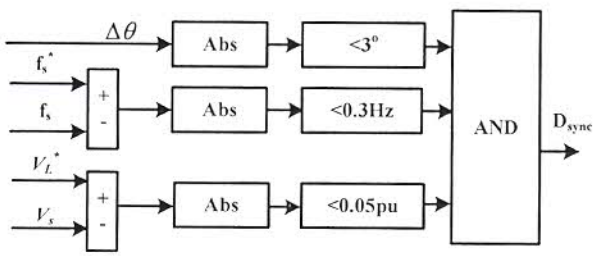

Fig. 4. Synchronization of PV-B-DSTATCOM

D. Reference Generation for PV-B-DSTATCOM

The PV-B-DSTATCOM operates in current control mode in grid connected mode of operation and in voltage control mode in standalone mode of operation.

The major objective in grid connected mode is to inject PV array power into grid and also maintain grid current sinusoidal and at unity power factor by compensating load current quality issues. The fundamental positive sequence component (FPSC)

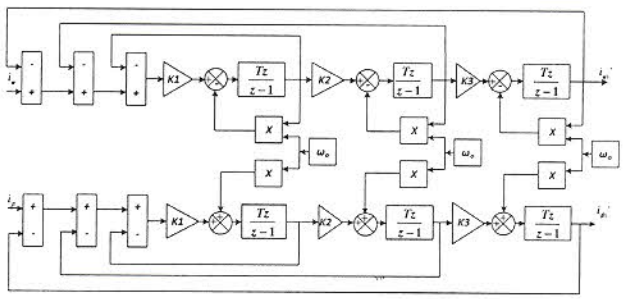

Fig. 5. Structure of Third Order Complex Band Pass Filter

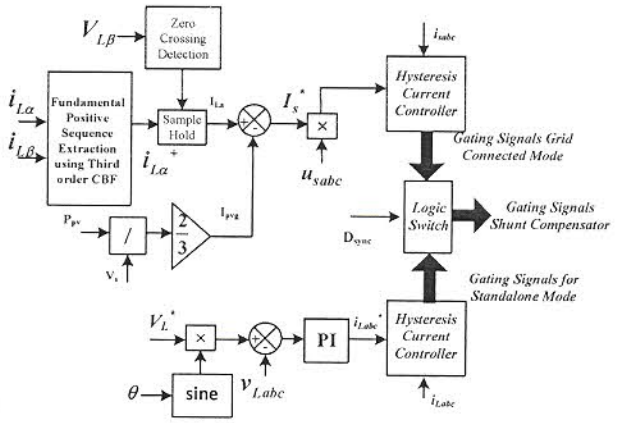

Fig. 6. Synchronization of PV-B-DSTATCOM

of the three phase nonlinear load current is obtained using a third order complex band pass filter (CBF)[11]. The input to the filter is load current in $\alpha - \beta$ domain. The output of the filter is FPSC of load current in $\alpha - \beta$ domain. The α component of load current FPSC is sampled at the zero crossing of the β component of the load voltage, which gives the magnitude of the active component I_{La}. The grid current component corresponding to the PV array power is obtained by the following equation

$$I_{pvg} = \frac{2}{3}\frac{P_{pv}}{V_s} \tag{1}$$

The magnitude of reference grid current is obtained as

$$I_s = I_{La} - I_{pvg} \tag{2}$$

The reference grid current magnitude I_{La} is multiplied with grid voltage templates (u_{sabc}) to generate instantaneous reference signals which is then passed through the hysteresis current controller to generate gating signals for PV-B-DSTATCOM during grid connected mode of operation.

When the grid is not available, the PV-B-DSTATCOM operates in voltage control mode. The phase of the voltages is generated through phase generation logic. This is then multiplied with reference magnitude of load voltage (V_L^*) to generate reference voltages for each phase. The error between reference voltages of each phase and sensed voltages are given to PI controllers which then generates reference load currents for each phase. The reference load currents are compared with sensed load currents in a hysteresis controller to generate gating signals during standalone mode of operationg.

The gating signals for standalone mode and grid connected mode are then passed through a switch control logic which then decides the output signals based on the synchronization signal D_{sync}.

IV. Simulation Performance of PV-B-DSTATCOM System

The PV-B-DSTATCOM system is tested in Matlab-Simulink software for its performance under various conditions such as transition from standalone mode of operation to grid connected mode of operation, irradiation change, and load unbalance conditions. The behavior of the system under these conditions are explained in the following sections

A. Synchronization performance of PV-B-DSTATCOM

The operation of PV-B-DSTATCOM during transition from standalone mode to grid connected mode and vice versa is presented in Fig. 7. The signals captured are v_{sabc}, v_{Labc}, V_{dc} , synchronization signal (D_{sync}), phase angle of load and PCC voltages ($\theta_{L,S}$), i_{sabc}, i_{Labc}, I_{pv}, I_{bt}, V_{bt}. Initially the grid is not available and the PV-B-DSTATCOM is operating in standalone mode of operation. The PV array supplies power to the load while the remaining power is being stored in the battery bank. When the grid becomes available at 0.2s, the synchronization logic tries to synchronize the PV-B-DSTATCOM voltage with PCC Voltages, once all the conditions for synchronization are met, the syncrhonization logic generates D_{sync} which turns on the PES and connects the grid with the PV-B-DSTATCOM system, and the system starts feeding PV power into grid along with compensation of load current quality issues. It can be observed that during this condition, the battery bank operates in nearly floating condition compensating for the only the loss component of the system. At t=0.5s, the grid becomes unavailable and the PV-B-DSTATCOM changes to standalone mode of operation. During this entire period, the load gets uninterrupted supply of power.

B. PV-B-DSTATCOM response during Load Unbalance Condition

The response of PV-B-DSTATCOM during the removal of a load phase is presented in Fig.8. The signals shown are v_{sabc}, v_{Labc}, V_{dc}, i_{sabc},i_{Labc}, i_{SHabc}, G, I_{pv}, P_{pv}, V_{BT}, I_{BT}.

The system is operating in grid connected mode with solar irradiation at $1000W/m^2$. At t=0.3s, phase 'b' of the load is removed causing an unbalanced three phase load condition. The shunt compensator compensates for the unbalanced load

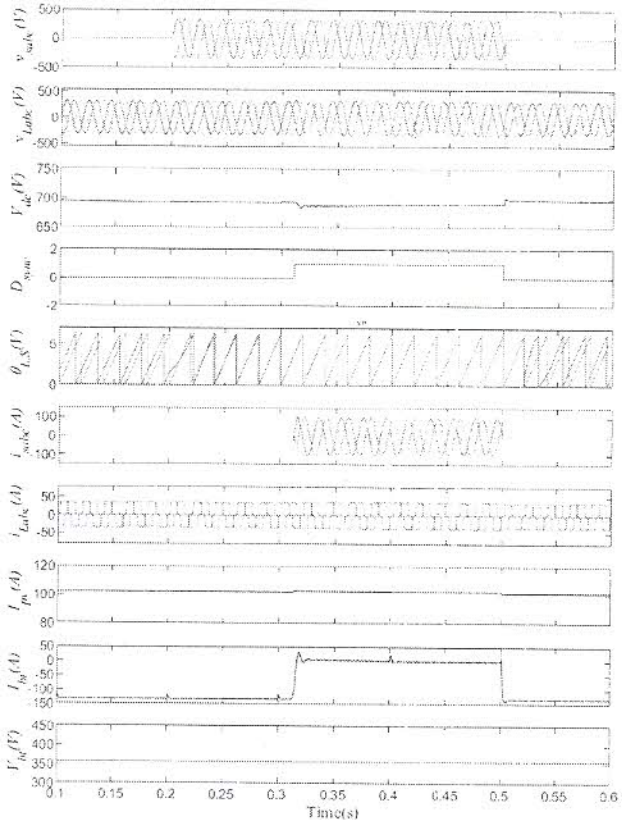

Fig. 7. Synchronization Performance of PV-B-DSTATCOM

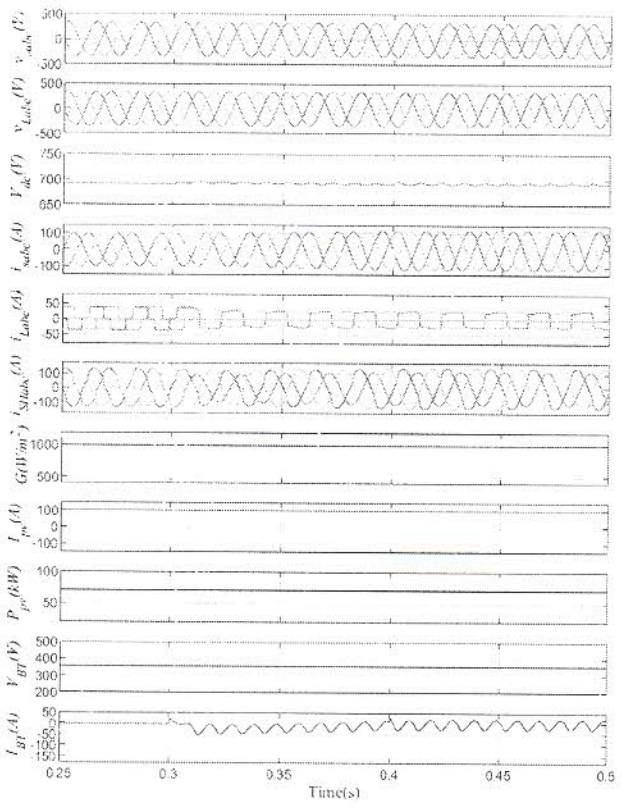

Fig. 8. Response of PV-B-DSTATCOM during Load Unbalance Condition

condition and maintains the grid current balanced as well as sinusoidal. There is double harmonic ripple in the DC-link voltage due to the double harmonic content in the power flow during unbalanced condition. The battery current is having double harmonic content with average nearly zero as the DC-link voltage is maintained by the battery bank along with bi-directional controller. The double harmonic content in the DC-link voltage is reflected in the battery current.

C. Response of PV-B-DSTATCOM during Variation in Solar Irradiation Condition

The behavior of PV-B-DSTATCOM is checked under condition of irradiation variation under both grid connected mode and standalone mode of operation which are presented in Fig. 9 and Fig.10. The signals captured are v_{sabc}, V_{dc}, v_{Labc}, i_{sabc}, i_{Labc}, i_{SHabc}, G, I_{pv}, P_{pv}, V_{BT}, I_{BT}.

In grid connected mode, the battery power is not utilized for load power. Hence, when irradiation decreases from G=1000W/m^2 to G=500W/m^2, the grid current reduces due to the reduction in power available to supply to the grid. The battery current is negligible and DC-link voltage is regulated at its desired voltage point. In standalone mode of operation as seen in Fig.10, the PV array and battery bank system is used to supply the load power. The excess PV power is stored in the battery bank system. Initally, battery charging current is -120 A, but when the solar irradiation is changed from G=1000W/m^2 to G=500W/m^2 between 0.2 s to 0.4s, the battery charging current decreases from -120 A to -20 A due to reduced availability of surplus power. The load voltage is regulated at its desired value of 415V. The total harmonic distortion (THD) of the grid current and load current is presented in Fig.11. It can be observed that even thought the load current current is non-linear with a THD of 24.86%, the grid current is having a THD of 1.9% thereby meeting the requirements of IEEE-519 standard.

V. Conclusion

The performance of the PV-B-DSTATCOM system has been extensively analyzed through simulation in Matlab-Simulink Software. This system has capability to operate both in grid connected condition as well as in standalone mode of operation when grid is not available. The transition between the standalone mode of operation and grid connected mode of operation is seamless and thereby enabling uninterruptible operation of critical loads. The system behavior has been tested under different dynamic conditions such as load unbalance, transition between grid connected mode and standalone mode and vice-versa. The grid current of the compensated system is in conformance with the limits prescribed in IEEE-519 standard.

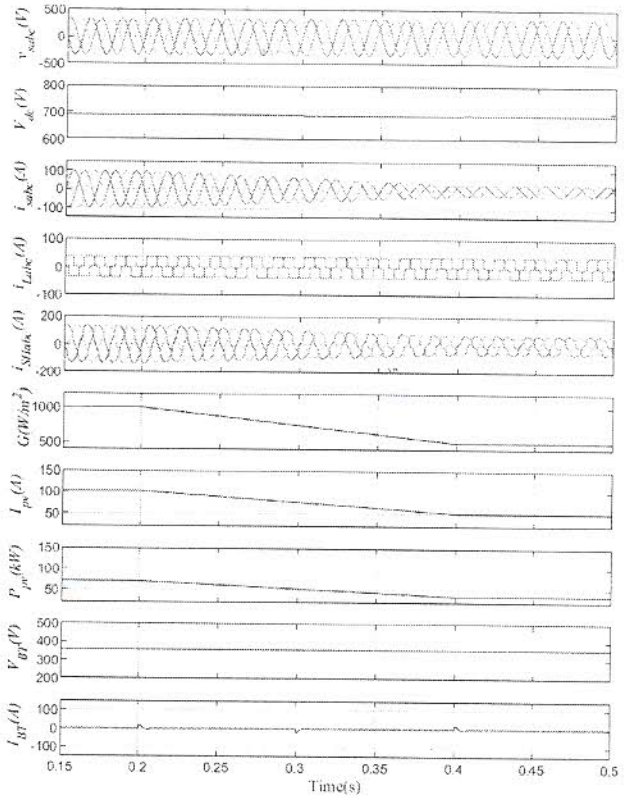

Fig. 9. PV-B-DSTATCOM Behavior During Irradation Change

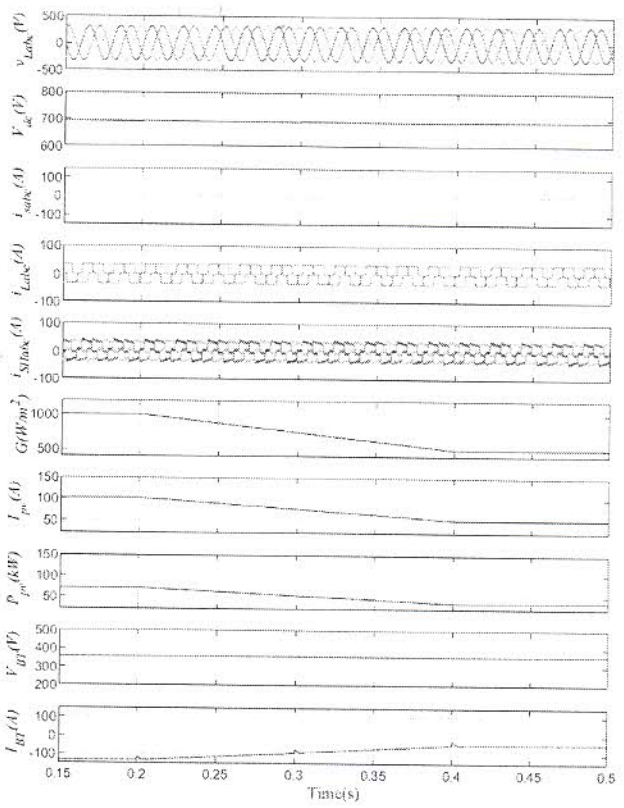

Fig. 10. PV-B-DSTATCOM Behavior During Irradation Change in Standalone Mode

ACKNOWLEDGMENT

Authors would like to thank Science & Engineering Research Board (SERB), Department of Science & Technology (DST), Govt. of India, for supporting this work under Grant Number: EMR/2017/004188.

APPENDIX

Simulation Parameters: Supply System: 415V,50Hz
Load: Nonlinear load 15 Ohm, 150mH
Bidirectional Converter Inductor: 4mH
DC-link Capacitor: 15mF
PV-B-DSTATCOM Inductor: 2 mH
, Ripple Filter :C_f=10μF, R_f=10Ω
PI gains of DC-link controller:K_P=25,K_I=0.01,
DC-bus Voltage: 700 V
PV Array Rating:
V_{oc} = 864V, V_{mpp} = 695V ,I_{sc}=107.4A, I_{mpp} = 101 A, P_{pv} = 70.8kW;
Battery Bank: 360 V, 6000Ah, Battery Type: Lead Acid

REFERENCES

[1] Z. Ali, N. Christofides, L. Hadjidemetriou, and E. Kyriakides, "Multi-functional distributed generation control scheme for improving the grid power quality," *IET Power Electronics*, vol. 12, no. 1, pp. 30–43, 2019.

[2] K. M. Reddy and B. Singh, "Multi-objective control algorithm for small hydro and spv generation-based dual mode reconfigurable system," *IEEE Transactions on Smart Grid*, vol. 9, no. 5, pp. 4942–4952, Sep. 2018.

[3] A. Sangwongwanich and F. Blaabjerg, "Mitigation of interharmonics in pv systems with maximum power point tracking modification," *IEEE Transactions on Power Electronics*, vol. 34, no. 9, pp. 8279–8282, Sep. 2019.

[4] S. Devassy and B. Singh, "Implementation of solar photovoltaic system with universal active filtering capability," *IEEE Transactions on Industry Applications*, vol. 55, no. 4, pp. 3926–3934, July 2019.

[5] R. Kumar, B. Singh, R. Kumar, and S. Marwaha, "Recognition of underlying causes of power quality disturbances using stockwell transform," *IEEE Transactions on Instrumentation and Measurement*, pp. 1–1, 2019.

[6] X. Guo, W. Wu, and Z. Chen, "Multiple-complex coefficient-filter-based phase-locked loop and synchronization technique for three-phase grid-interfaced converters in distributed utility networks," *IEEE Transactions on Industrial Electronics*, vol. 58, no. 4, pp. 1194–1204, April 2011.

[7] P. K. Ray and B. Subudhi, "A vllms based harmonic estimation of distorted power system signals and hybrid active power filter design," in *2013 IEEE 10th International Conference on Power Electronics and Drive Systems (PEDS)*, April 2013, pp. 104–108.

[8] P. Garanayak, G. Panda, and P. K. Ray, "Power system harmonic parameters estimation using adaline-vllms algorithm," in *2015 International Conference on Energy, Power and Environment: Towards Sustainable Growth (ICEPE)*, June 2015, pp. 1–6.

[9] T. Tran, T. Chun, H. Lee, H. Kim, and E. Nho, "Pll-based seamless transfer control between grid-connected and islanding modes in grid-connected inverters," *IEEE Transactions on Power Electronics*, vol. 29, no. 10, pp. 5218–5228, Oct 2014.

[10] G. G. Talapur, H. M. Suryawanshi, R. R. Deshmukh, M. S. Ballal, and R. Choudhary, "Hybrid control technique for load sharing and seamless transition in microgrid mode of operation," in *2018 IEEE International*

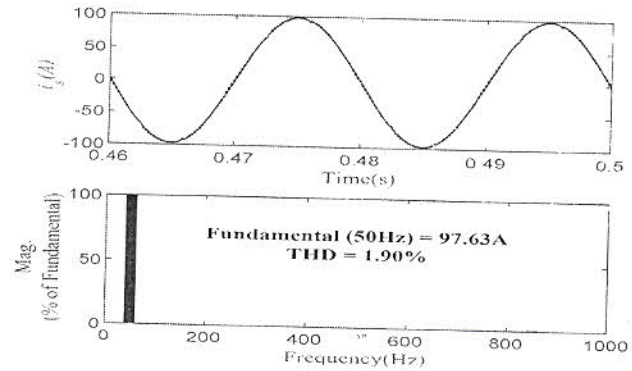

(a) Harmonic Spectra of Grid Current

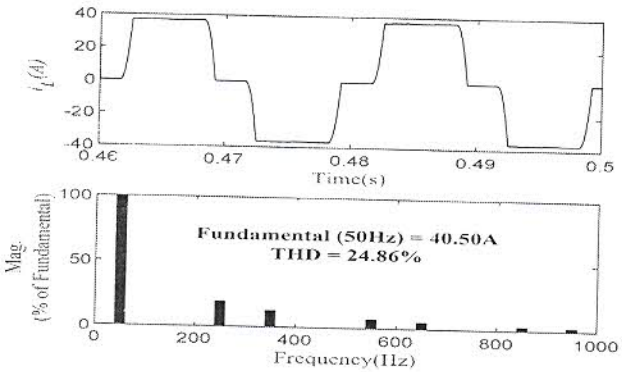

(b) Harmonic Spectra of Load Current

Fig. 11. Current Harmonic Spectra

Conference on Power Electronics, Drives and Energy Systems (PEDES), Dec 2018, pp. 1–6.

[11] S. Golestan, F. D. Freijedo, and J. M. Guerrero, "A systematic approach to design high-order phase-locked loops," *IEEE Transactions on Power Electronics*, vol. 30, no. 6, pp. 2885–2890, June 2015.